

Numerical Investigation of Flow Features in Turbulent Channel Flow under Stratified and Neutral Conditions

Steven A. Thompson¹ and Reetesh Ranjan.²

*Department of Mechanical Engineering, The University of Tennessee Chattanooga
615 McCallie Ave, Chattanooga, Tennessee, 37403, USA*

The presence of density stratification adds to the complexity of turbulence by affecting the small-scale mixing, the large-scale circulation, and the inter-scale interactions. The density in underwater naval flows depends upon temperature and salinity scalars. A key feature of such flows is the presence of internal waves, which affect its spatio-temporal dynamics. In this study, the spectral and modal characteristics of turbulent channel flow under stably stratified and neutral conditions are examined. We analyze direct numerical simulation datasets at a frictional Reynolds number of 395 and the frictional Richardson number of 0 (neutral) and 60 (stratified). First, the two-dimensional spectra of fluctuations in the vertical velocity, density, momentum flux, and buoyancy flux at different wall-normal planes are obtained to examine the role of buoyancy and shear-generated turbulence. Afterward, the presence of internal waves, a characteristic feature of stratified turbulent flows, is inferred in terms of the phase relationship between the vertical velocity and density fluctuations. Finally, the spatial and temporal structure of the internal waves is examined using the spectral proper orthogonal decomposition technique to obtain the dynamically relevant flow structures.

I. Introduction

Stably stratified turbulent flows are observed in various geophysical, environmental, and engineering flows, which has led to numerous studies in the past [1, 2, 3]. Particularly in the context of oceanography, the density of the water is dependent on two scalar fields, namely, the temperature and the salt content, or salinity of the water, which can be expressed through an equation of state (EoS). The differences in the molecular diffusivity of these scalar fields, which are characterized in terms of Lewis number ($Le = Sc/Pr$) lead to the occurrence of the differential diffusion phenomenon. Here, Sc and Pr denote the Schmidt and Prandtl numbers, respectively. While the computational investigation of stratified turbulent flows is challenging on its own due to the added complexity of the effects of density stratification on the turbulence characteristics, the computational complexity is increased further due to the presence of differential diffusion phenomenon and nonlinear dependence of density on temperature and salinity fields, which in turn affects the small-scale mixing, large-scale circulation and can lead to the onset of flow instabilities. In such flows, the difference in the molecular diffusion of temperature and salinity is at least two orders of magnitude ($Pr \sim O(1)$, $Sc \sim O(10^2)$), which requires excessive computational resources to accurately capture the spatio-temporal dynamics of the evolution of the scalar fields. Therefore, efficient and robust models are needed for the numerical investigation of such flows in practical scenarios. To this end, direct numerical simulation (DNS) [4, 5, 6] can be used as a tool to examine the fundamental aspects of stratified turbulence, which can facilitate the development of novel and/or improvement of existing models for efficient prediction of such flows.

Past DNS-based studies have examined the effects of stable density stratification on turbulent flows with a mean shear by considering both homogeneous [7] and non-homogeneous [4, 8, 6] flows. The two key parameters governing such flows include the Reynolds number (Re), which characterizes the state of turbulence, and the Richardson number (Ri), which characterizes the level of stable stratification. These studies have shown that with an increase in Ri the

¹ Graduate Research Assistant, Department of Mechanical Engineering, AIAA Student Member, AIAA Membership Number: 1603370

² Assistant Professor, Department of Mechanical Engineering, AIAA Senior Member, AIAA Membership Number: 480307

Student Category: Masters

turbulent mixing along the direction of stratification tends to decrease. Additionally, several physical flow features occur in such flows, which are much different from the unstratified (neutral) turbulent flows. Some of these features include the presence of internal waves, counter-gradient turbulent transport of momentum and density fields at different scales, increased level of anisotropy, disruption to the energy transfer across scales, modifications to coherent structures, Ri -dependent modifications to turbulent kinetic energy production and dissipation. Such flows can be classified into different regimes, which include the buoyancy-affected turbulence regime, buoyancy-dominated regime, and buoyancy-controlled regime. Past studies have analyzed such regimes by varying the governing parameters (Re and Ri) and have performed scaling analysis to characterize the state of the stratified turbulence in terms of, for example, the effects of buoyancy on structural and spectral features, the role of shear strength and the buoyancy on stability, etc. However, there are limited studies focused on examining the effects of differential diffusion while employing a nonlinear EoS on these flow features under non-homogeneous flow conditions with a mean shear.

In the present study, we focus on the widely studied turbulent channel flow configuration under neutral and stratified conditions. In this canonical flow, the presence of density stratification affects the flow features in the near-wall region as well as the outer region. Although the configuration is geometrically simpler, it exhibits the presence of a wide range of turbulence physics, which include the presence of two competing mechanisms, namely, one responsible for the generation of turbulence by the extraction of turbulent kinetic energy from the mean shear and the other suppressing turbulence due to stratification by the conversion of kinetic energy to potential energy. Past studies of this flow [4, 8, 6] have shown that with an increase in the level of stable density stratification, the skin friction coefficient (C_f) and Nusselt number (Nu), tend to reduce. In addition, interfacial wave-like motions, referred to as internal waves, exist in the outer/core region of the flow, where strong counter-gradient turbulent momentum and density fluxes are observed. Moreover, in the regions of flows (particularly the outer region), where the length scales are large and the shear is weak, the density stratification suppresses the turbulent transport along the direction of stratification. The effects of differential diffusion while using a nonlinear EoS to determine density from temperature and salinity fields on the aforementioned flow features have not been extensively studied in the past. Therefore, we simulate a fully developed turbulent channel flow at a frictional Reynolds number (Re_τ) of 395 and frictional Richardson number (Ri_τ) of 0 (neutral) and 60 (stratified) to complement the findings of past studies. A particular focus of this study is on examining the spectral and modal characteristics of the flow features in this configuration.

This article is arranged as follows. The mathematical formulation and numerical methodology are discussed in Sec. II. The details of the computational setup are presented in Sec. III. The results are discussed in Sec. IV. Finally, in Sec. V, a summary of the findings of this study and an outlook for the future are presented.

II. Mathematical Formulation and Numerical Approach

In this section, we first describe the governing equations. Afterward, we present the numerical strategy considered in this study.

A. Governing Equations

The equations listed below show the incompressible Navier-Stokes equations that govern the stratified turbulent flows considered in this study.

$$\frac{\partial u_i}{\partial x_i} = 0, \quad (2.A.1)$$

$$\frac{\partial u_i}{\partial t} + \frac{\partial u_i u_j}{\partial x_j} = -\frac{1}{\rho_0} \frac{\partial p}{\partial x_i} + \nu \frac{\partial^2 u_i}{\partial x_j \partial x_j} - \delta_{i3} \frac{\rho_f}{\rho_0} g, \quad (2.A.2)$$

$$\frac{\partial \rho_T}{\partial t} + \frac{\partial \rho_T u_j}{\partial x_j} = k_T \frac{\partial^2 \rho_T}{\partial x_j \partial x_j}, \quad (2.A.3)$$

$$\frac{\partial \rho_S}{\partial t} + \frac{\partial \rho_S u_j}{\partial x_j} = k_S \frac{\partial^2 \rho_S}{\partial x_j \partial x_j}. \quad (2.A.4)$$

The above equations account for the mass conservation, momentum balance, and transport equations for the salinity and temperature fields. Here, u_i refers to the velocity component, ρ_t denotes the density, ρ_T denotes the temperature, ρ_S denotes the salinity, p refers to pressure deviation, ν is kinematic viscosity, and k_T and k_S are the molecular diffusivities of temperature and salinity fields, respectively. The density of the flow is determined using a nonlinear approximation Equation of State (EoS) of the UNESCO EoS [9]. The approximation is linear with respect to salinity and nonlinear with respect to temperature and is expressed as

$$\rho_t(\rho_T, \rho_S) = \rho_0 + (c_1 + c_2\rho_T + c_3\rho_S + c_4\rho_T^2 + c_5\rho_S\rho_T + c_6\rho_T^3 + c_7\rho_S\rho_T^2) \quad (2.A.5)$$

$$\rho_t(x_1, x_2, x_3, t) = \rho_0 + \rho_b(x_3, t) + \rho_f(x_1, x_2, x_3, t) \quad (2.A.6)$$

$$\rho_b = \langle \rho_t - \rho_0 \rangle \quad (2.A.7)$$

The coefficients, c_n for $n = 1 \dots 7$, are the values multiplying each term of the nonlinear approximation. The method of solving for the coefficients is derived by a previous study [9]. ρ_b , ρ_f , and ρ_0 represents the bulk density, density fluctuations, and the reference density. The bulk density is found using $\langle \rho_t - \rho_0 \rangle$, taking the difference in total density at all points from the reference density and then averaging over planes parallel to the channel. Here, x_i with $i = 1, 2$, and 3 denotes the Cartesian coordinate. The governing equations are complete after the specification of initial and boundary conditions.

B. Numerical Methods

The governing equations described in Sec. II A is solved using a parallel incompressible flow solver with primitive variable formulation using the artificial compressibility method and generalized curvilinear coordinates [10, 11, 12]. The solver is fourth-order accurate in space and second-order accurate in time and has been extended to account for stratification and different types of equations of states for density fluctuations [13]. The solver has been established in previous research to be an accurate approach for DNS and large-eddy simulation (LES) of turbulent flows [10, 11, 12] with and without density stratification [13]. The parallelization of the flow solver is performed using a standard domain-decomposition based technique leveraging the message passing interface (MPI) library.

III. Problem Description

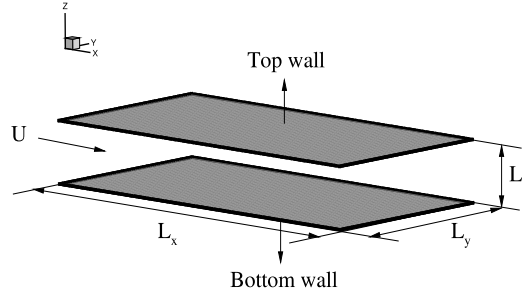


Figure 1 Schematic of the computational setup corresponding to periodic turbulent channel flow.

A schematic of the computational domain of the fully developed periodic channel flow considered in this study is shown in Fig. 1. The dimensions of the channel are $L_x = 2\pi h$, $L_y = \pi h$, and $L_z = 2h$ in the streamwise (x), spanwise (y), and vertical (z) directions, respectively. The top and bottom walls of the channel use a no-slip boundary condition, while a periodic boundary condition is used in other directions. Salinity and temperature boundary conditions are enforced along the top and bottom walls to ensure stable stratification in the vertical direction while utilizing the nonlinear EoS. A stable stratification implies higher density at the bottom and lower density at the top.

The flow is simulated at a fixed Re_τ of 395. Two different levels of stable density stratification are considered, which are specified in terms of Ri_τ . Specifically, a value of 0 and 60 are considered for Ri_τ , which implies neutral (no stratification) and stable stratification. To examine the effects of a moderate differential diffusion, two cases are considered where temperature and salinity scalars diffuse at different rates by modifying the values of Sc . Table 1 summarizes the major differences in the simulated cases. Cases N and S refer to the neutral and stratified cases that do not use differential diffusion and will be used to demonstrate the impact of stratification on the flow features that develop. Case S_D refers to the stratified differential diffusion case and will be used alongside case S to show the impact of differential diffusion on the flow features. Note that Case S_D has a finer mesh in comparison to the other cases due to the difference in Sc , where a finer mesh is required to ensure accurate capturing of the spatio-temporal dynamics of the salinity field. After the flow reaches a statistically stationary state based on Re_τ , time- and spanwise-averaged

statistics are obtained to examine the flow features that develop. All of these simulations have been performed using the high-performance computing (HPC) resources available from the University of Tennessee Chattanooga (UTC) Research Institute.

Table 1: Description of cases considered in this study.

Case	$N_x \times N_y \times N_z$	Ri_τ	Differential Diffusion
N	256 x 256 x 192	0	No ($Pr = 1, Sc = 1$)
S	256 x 256 x 192	60	No ($Pr = 1, Sc = 1$)
S _D	512 x 512 x 384	60	Yes ($Pr = 1, Sc = 4$)

IV. Results and Discussion

A. Mean Flow Features

The wall-normal variation of the mean flow field is shown in Fig. 2 in terms of the streamwise velocity, total density, temperature, and salinity fields. It is evident from these results that the effect of stratification is much more pronounced compared to the profiles obtained for the neutral case. Specifically, the mean streamwise velocity is an increase in the bulk velocity, which is a key effect of stable stratification [13, 4]. The effects of differential diffusion tend to be minor, with a reduction in the bulk velocity compared to the stratified case with no differential diffusion.

The normalized density profile shown in Fig. 2(b) shows a severe density gradient at the channel center under the stratified condition, as opposed to the gradual density change across the whole channel that can be seen with the neutral case. The sudden density change is caused by the formation of a pycnocline in the presence of stratification. This pycnocline essentially acts as a divide between the lower and upper halves of the channel. The neutral case does not form a pycnocline, which aligns with the observed behavior of a smooth, gradual density change between the channel walls due to vertical turbulent mixing [13, 8]. The case with differential diffusion, i.e., Case S_D, shows the same overall behavior, varying very little from the stratified non-differential diffusion case.

Figure 2(c) shows the profile of the normalized temperature, where the presence of stable density stratification leads to a sharp temperature gradient at the channel center, while the neutral case shows gradual change, which aligns with the behavior of the normalized density. This behavior is analogous to the variation of the total density in the vertical direction. As expected, the presence of differential diffusion does not have any observable impact on the vertical variation of normalized temperature. Note that both case S and S_D have the same value of Pr , so the diffusion rate of the temperature field is the same between cases, although one can expect some effect as the active scalar fields do affect the evolution of the flow field as well. The effect of differential diffusion is noticeable in the vertical variation of the normalized salinity field. The neutral and stratified cases show behavior that has been observed previously. Case S_D shows more severe salinity gradients near the channel walls and the channel center while remaining nearly constant in the regions between the walls and the center. This is expected since the different diffusion rates are applied by altering the Schmidt number, which in turn causes the salinity of the flow to diffuse more easily in the vertical direction.

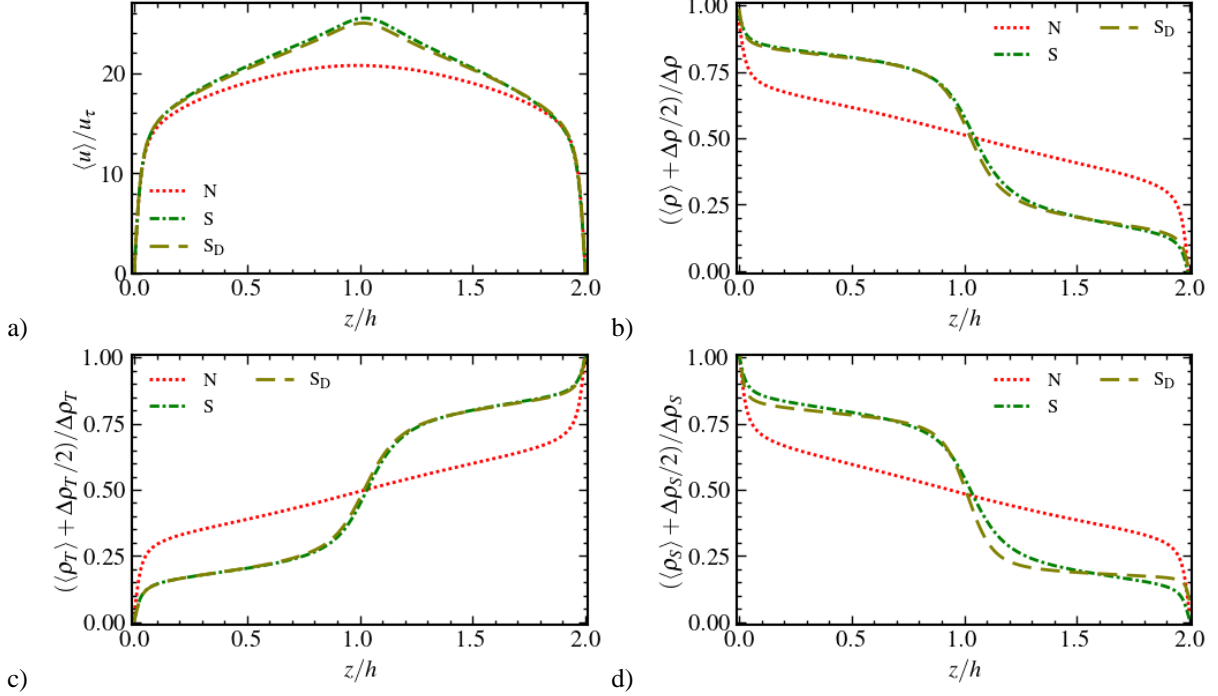


Figure 2: Wall-normal profile of mean streamwise velocity (a), density (b), temperature (c), and salinity (d) fields.

B. Two-Dimensional Spectra

To examine the effects of density stratification and differential diffusion on length-scales of the flow field, we examine the two-dimensional (2D) spectra of the normalized buoyancy flux ($\frac{\rho' w'}{\rho_\tau u_\tau}$), density fluctuations ($\frac{\rho'}{\rho_\tau}$), momentum flux ($\frac{u' w'}{u_\tau^2}$), and vertical turbulent kinetic energy ($\frac{w' w'}{u_\tau^2 h}$) at different wall-normal locations. These spectra are dependent on a 2D wavelength $\lambda = (\lambda_x, \lambda_y)$. Figures 3 and 4 show the 2D spectra at $z^+ = 300$ and 395. In both figures, the contour lines are representative of the energy at the chosen wavelength in relation to the maximum for the 2D spectra for the case, where each section represents 20%, 40%, 60%, or 80% of the maximum. The contour region, solid line, and dotted line represent cases N, S, and S_D , respectively.

The presence of stratification can lead to a concentration in the wave number, as observed in Fig. 3, where the density spectra concentrate towards higher wavelengths in the streamwise direction [14]. The spectrum of vertical kinetic energy also shows a similar trend where λ_x is slightly contracted toward the lower wavelengths, while the neutral case is spread over wider wavelengths. The vertical kinetic energy shows two concentrated regions for the stratified case, which can be caused by the presence of turbulence and internal waves [14]. Differential diffusion was shown to have a minor impact on the 2D spectra in this region. It leads to a shift in the buoyancy flux away from lower wavelengths. The density spectra show a diffusion in the wavelength concentration, where it spreads across a range of wavelengths and matches the behavior shown for the neutral case. This can possibly be due to the effects of differential diffusion on the density field, which was also observed in terms of the effect on the density field, as observed in Fig. 2(d). The spectrum of vertical kinetic energy shows a concentration in the energy spectra for higher wavelength, i.e., λ_y , but it can be observed that the presence of stratification causes the concentration to shift toward the longer streamwise wavelength. Overall, we can observe that an increase in the anisotropy of the spectra of various quantities tends to occur in the stratified cases where noticeable effects of differential diffusion are also prevalent.

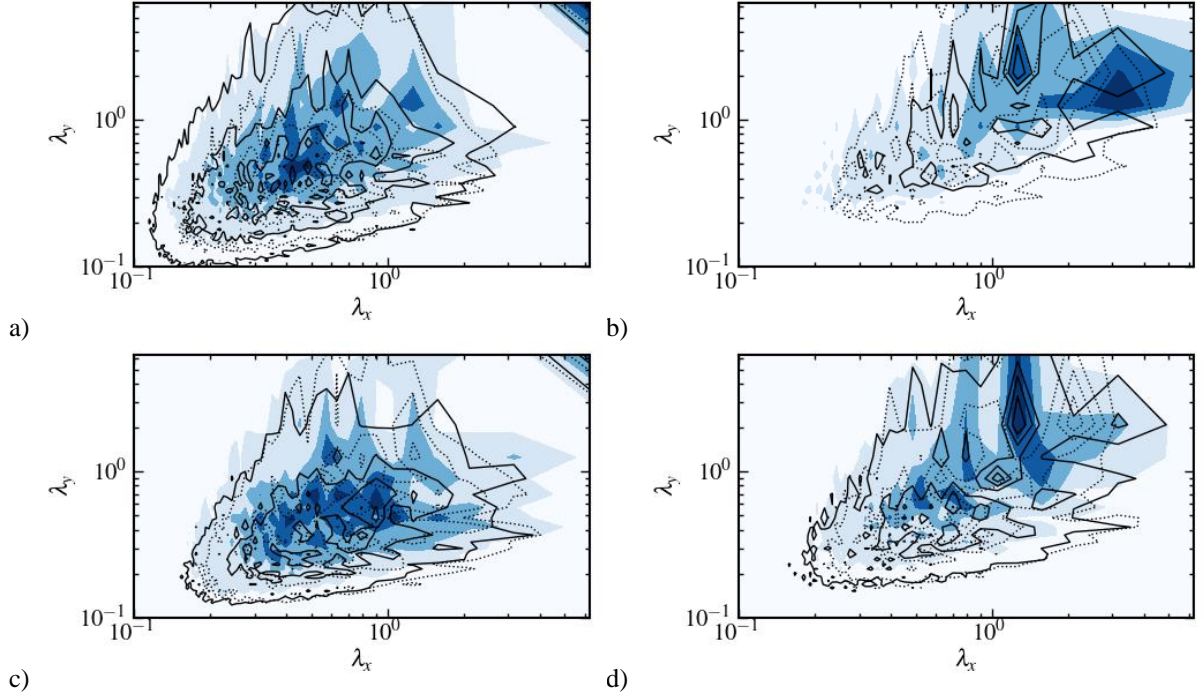


Figure 3: 2D pre-multiplied spectra of buoyancy flux (a), density (b), momentum flux (c), and vertical kinetic energy (d) at $z^+ = 300$. Shaded contour, dashed line, and solid line represent cases N, S, and S_D , respectively.

Figure 4 shows the 2D spectra of various quantities at the channel center, i.e., $z^+ = 395$. The presence of stratification leads to a further narrowing of the range of λ_x where higher values of the fluctuations of density and flow field tend to occur. This clearly shows that the impact of stratification on the spectra is much more significant near the channel center where the pycnocline formation occurs compared to the location within the core of the channel away from the center. The density and vertical kinetic energy spectra for stratified cases show a peak in two regions at $z^+ = 300$. However, the concentration at the lower wavelengths has been suppressed at the channel center, and the spectra have been concentrated toward the high wavelengths. This suppression and concentration would indicate the presence of internal waves at the channel center. Similar to Fig. 3, the presence of differential diffusion shifts these peaks toward the higher streamwise wavelengths. The buoyancy and momentum flux spectra show a contraction towards the lower streamwise wavelengths in cases with stratification. As expected, the spectra of the neutral case show little change between Figs. 3 and 4, indicating the impact of turbulence on the energy spectra is consistent in these regions of the channel.

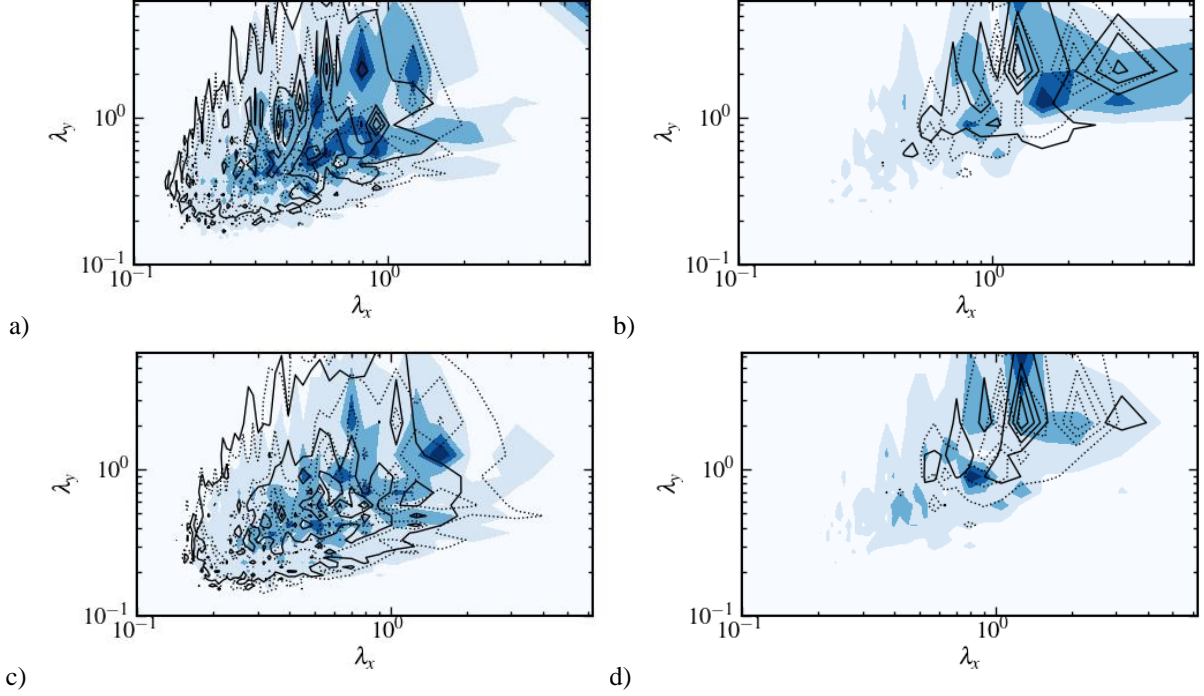


Figure 4: 2D spectra of buoyancy flux (a), density (b), momentum flux (c), and vertical kinetic energy (d) at the channel center, $z^+=395$. Shaded contour, dashed line, and solid line represent N, S, and S_D , respectively.

C. Internal Waves

The presence of internal waves is a key feature of stratified turbulent flows. Such waves can be inferred from the phase relationship of the vertical velocity and the density fluctuations. It is defined as $\theta_{\rho w}(k_x, z, t) = \tan^{-1}\left(\frac{Qu_{\rho w}(k_x, z, t)}{Co_{\rho w}(k_x, z, t)}\right)$, where $Qu_{\rho w}$ and $Co_{\rho w}$ are the quad-spectrum and co-spectrum of $\rho'w'$ and k_x is the wave number in the streamwise direction. The magnitude of the phase angle determines the direction of density flux, where $\theta_{\rho w} = 0^\circ$ indicating the presence of shear-driven vertical density flux while $\theta_{\rho w} = \pm 180^\circ$ indicates flux reversal due to buoyancy-driven counter gradient buoyancy flux. $\theta_{\rho w} = \pm 90^\circ$ indicates the presence of internal waves due to the lack of this vertical density flux in either direction [13]. Fig. 5 compares the phase angle of the cases to show the impact of stratification and differential diffusion near the channel wall, $z^+ = 10$, and the channel center, $z^+ = 395$.

Figures 5(a) and 5(c) show the phase angle in the near wall region. It can be observed that lower wavenumbers possess phase angles of $\theta_{\rho w} = 0$ and $\theta_{\rho w} = \pm 180^\circ$ at high wave numbers, indicating the presence of vertical buoyancy flux near the wall. The dominance of $\theta_{\rho w} = 0^\circ$ at the lower energetic wave numbers indicates the shear-driven density flux is dominant and has little dependence on stratification and differential diffusion near the wall [13]. Figure 5(b) shows that, at the channel center, the presence of stratification leads to a phase angle of $\theta_{\rho w} = -90^\circ$ for most wave numbers, while the neutral case primarily has a phase angle of $\theta_{\rho w} = 0^\circ$. The shift in phase angle from $\theta_{\rho w} = 0^\circ$ to $\theta_{\rho w} = -90^\circ$ shows that stratification suppresses the shear-driven vertical density flux in favor of internal waves [8]. Figure 5(d) shows that there is little difference in phase angle for the lower energetic wavenumbers. A difference can be observed at high wavenumbers, where case S_D shows a phase angle of $\theta_{\rho w} = \pm 180^\circ$ while Case S never does, showing that only Case S_D shows the presence of buoyancy-driven counter-density flux.

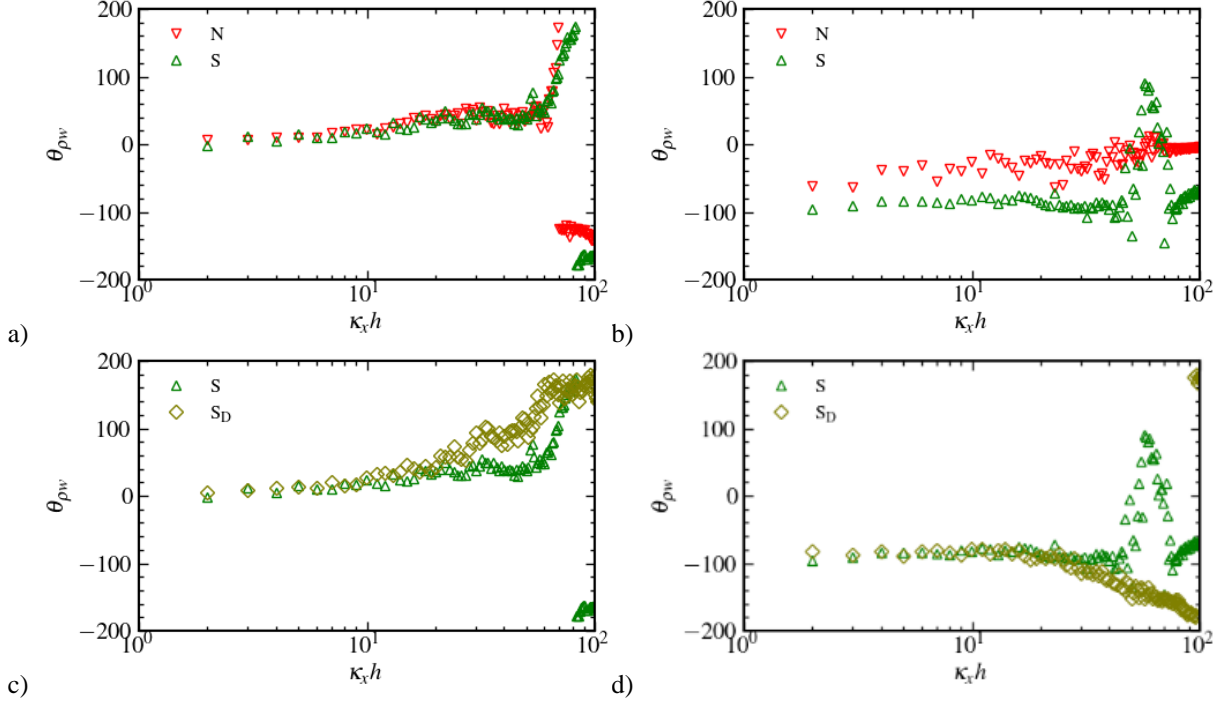


Figure 5: Phase angle at $z^+=10$ (a, c) and at $z^+=395$ (b, d) comparing the impact of stratification (a, b) and differential diffusion (c, d).

D. Coherent Flow Features

Now, we examine the dynamics of coherent flow features using the spectral proper orthogonal decomposition (SPOD) technique [15,16]. The resulting modes from SPOD analysis represent dominant spatial and temporal structures [15]. In this approach, the modes are associated with frequencies and can be utilized to observe how the flow structures change with time. It allows for the analysis of the type of flow features that occur in the flow, as well as the amount of energy they possess and their frequency.

Figure 6 shows the three highest energy modes for any given frequency for all the cases. It can be observed that there is a clear distinction in the modal energy in each case, with case S_D showing the greatest amount at any given frequency, followed by case S , then case N . As the frequency increases, a decrease in the energy of all modes can be observed.

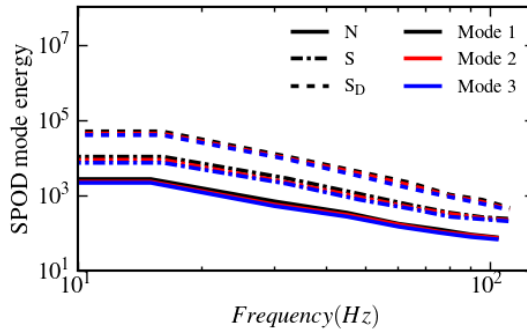


Figure 6: Modal energy of dominant modes at different frequencies.

Figure 7 shows the dominant modes for all the cases at two different frequencies for the density fluctuations of the flow. It can be observed that stratification and differential diffusion have an impact on the resulting dominant SPOD modes. In particular, the presence of stratification influences the shape of the modes. Between cases N and S , the modal shapes of the stratified show more defined structures. This difference in behavior may be tied to the presence

of turbulence in the neutral case and the presence of internal waves along with turbulence in the stratified case. The neutral case has higher levels of turbulent mixing at the channel center. However, the stratified cases show signs of the presence of internal waves, which is also evident from the phase angle relationship and the 2D energy spectra, as discussed before. The presence of stratification causes a suppression of turbulence at the channel center in the form of the formation of a pycnocline. This allows for modal shapes to capture the internal waves at the channel center through the long vertical structures. The presence of differential diffusion leads to the dampening of the modes, but the vertical structures tend to be similar to those observed in Case S, implying the role of internal waves.

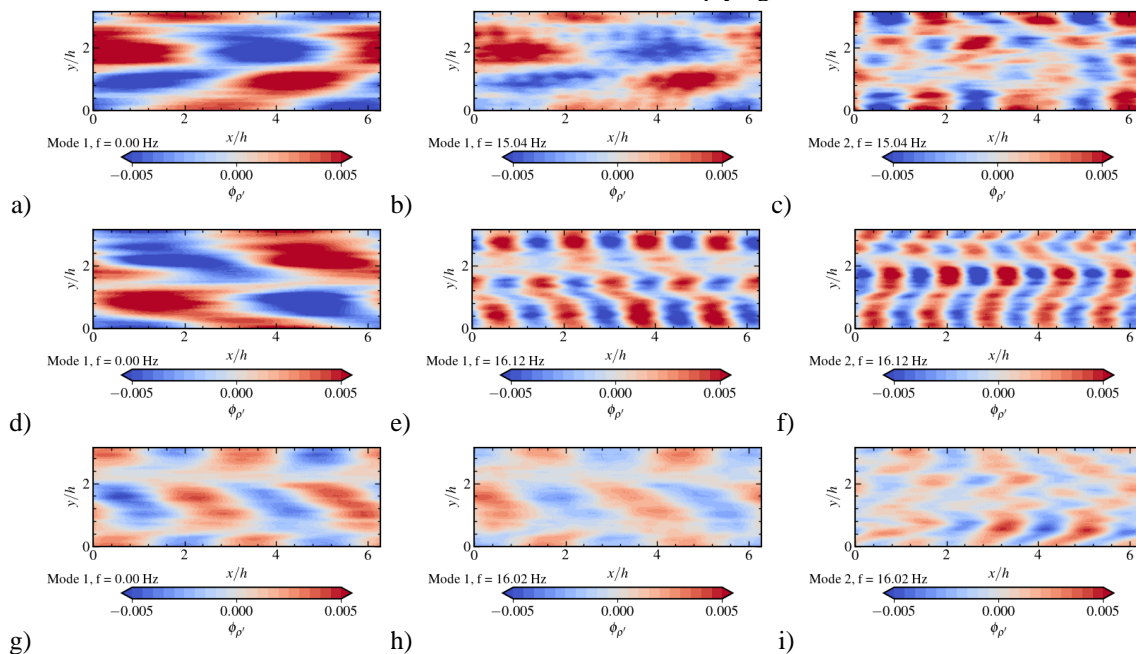


Figure 7: Dominant modes for the cases N (a, b, c), S (d, e, f), and Sd (g, h, i)

V. Conclusion

Density stratification in turbulent flows is observed in several applications. Therefore, the importance of investigating stratification and differential diffusion effects cannot be overstated. Specifically, in turbulent flows occurring within waterbodies, the flow density often depends upon temperature and salinity through a nonlinear EoS and has effects on differential diffusion. In the present study, DNS of stably stratified turbulent channel flow at $Re_\tau = 395$ was performed to examine the effects of stratification ($Ri_\tau = 0$ and 60) and differential diffusion ($Pr = 1$, and $Sc = 1$ and 4).

The analysis of the results shows that stable density stratification suppresses vertical turbulent mixing and leads to the appearance of large-scale internal waves. The presence of internal waves and their effects were examined through the phase angle relationship between vertical velocity and density fluctuations, the concentrations of the 2D energy spectra, and the shape of the dominant modes. The role of differential diffusion was evident from the vertical profile of density and the complex effects on the flow features that develop, such as the presence of counter gradient density flux at the channel center, the concentration of the density, and vertical kinetic energy spectra towards higher streamwise wavelengths, and the shape of the SPOD mode structures. In the future, we will leverage the results presented in this study to assess and improve the performance of models for efficient and reliable simulations of such flows in practical systems.

Acknowledgments

This work is supported in part by a CEACSE grant through the University of Tennessee at Chattanooga (UTC). The computational resources are provided by the UTC Research Institute under grants from the National Science Foundation (Grant Nos. 1925603 and 2201497) and are greatly appreciated.

References

- [1] Turner, J. S. (1979). Buoyancy effects in fluids. Cambridge university press. <https://doi.org/10.1017/CBO9780511608827>
- [2] Fernando, H. J. (1991). Turbulent mixing in stratified fluids. Annual review of fluid mechanics, 23(1), 455-493. <https://doi.org/10.1146/annurev.fl.23.010191.002323>
- [3] Grimshaw, R. (Ed.). (2002). Environmental stratified flows (No. 3). Springer Science & Business Media. ISBN: 0792376056, 9780792376057
- [4] García-Villalba M., del Álamo J.C.; Turbulence modification by stable stratification in channel flow. Physics of Fluids 1 April 2011; 23 (4): 045104. <https://doi.org/10.1063/1.3560359>
- [5] Gerz T, Yamazaki H. Direct numerical simulation of buoyancy-driven turbulence in stably stratified fluid. Journal of Fluid Mechanics. 1993;249:415-440. doi:10.1017/S0022112093001235
- [6] Garg, R. P., Ferziger, J. H., Monismith, S. G., & Koseff, J. R. (2000). Stably stratified turbulent channel flows. I. Stratification regimes and turbulence suppression mechanism. Physics of Fluids, 12(10), 2569-2594. <https://doi.org/10.1063/1.1288608>
- [7] Holt, S. E., Koseff, J. R., & Ferziger, J. H. (1992). A numerical study of the evolution and structure of homogeneous stably stratified sheared turbulence. Journal of Fluid Mechanics, 237, 499-539. doi: 10.1017/S0022112092003513
- [8] Armenio V., Sarkar S. An investigation of stably stratified turbulent channel flow using large-eddy simulation. Journal of Fluid Mechanics. 2002;459:1-42. doi:10.1017/S0022112002007851
- [9] Brydon, D., Sun, S., Bleck, R. (1999), A new approximation of the equation of state for seawater, suitable for numerical ocean models, J. Geophys. Res., 104(C1), 1537–1540, doi:10.1029/1998JC900059.
- [10] Kim, W.-W., Menon, S. (1999), An unsteady incompressible Navier–Stokes solver for large eddy simulation of turbulent flows. Int. J. Numer. Meth. Fluids, 31: 983-1017. [https://doi.org/10.1002/\(SICI\)1097-0363\(19991130\)31:6<983::AID-FLD908>3.0.CO;2-Q](https://doi.org/10.1002/(SICI)1097-0363(19991130)31:6<983::AID-FLD908>3.0.CO;2-Q)
- [11] Gungor A.G, Menon S., A new two-scale model for large eddy simulation of wall-bounded flows, Progress in Aerospace Sciences, Volume 46, Issue 1, 2010, Pages 28-45, ISSN 0376-0421, <https://doi.org/10.1016/j.paerosci.2009.10.001.m>
- [12] Ranjan R., Menon S. (2013) A multi-scale simulation method for high Reynolds number wall-bounded turbulent flows, Journal of Turbulence, 14:9, 1-38, DOI: 10.1080/14685248.2013.849382
- [13] Ranjan, R., Venkataswamy, M. K., and Menon, S., "Dynamic one-equation-based subgrid model for large-eddy simulation of stratified turbulent flows", Physical Review Fluids, vol. 5, no. 6, APS, 2020. doi:10.1103/PhysRevFluids.5.064601.
- [14] Lloyd C.J., Dorrell R.M., Caulfield C.P. The coupled dynamics of internal waves and hairpin vortices in stratified plane Poiseuille flow. Journal of Fluid Mechanics. 2022;934:A10. doi:10.1017/jfm.2021.1007
- [15] Nidhan S., Schmidt O.T., Sarkar S.. Analysis of coherence in turbulent stratified wakes using spectral proper orthogonal decomposition. Journal of Fluid Mechanics. 2022;934:A12. doi:10.1017/jfm.2021.1096
- [16] Schmidt, O. T., & Colonius, T. (2020). Guide to spectral proper orthogonal decomposition. Aiaa journal, 58(3), 1023-1033. <https://doi.org/10.2514/1.J058809>